24. O. M. Alifanov, "Some questions of solving inverse problems of heat conduction and of automated data processing in thermophysical investigations," Inzh.-Fiz. Zh., 39, No. 2, 211-219 (1980).
25. S. A. Budnik, "The problem of planning thermal measurements," Inzh.-Fiz. Zh., 39, No. 2, 225-230 (1980).
26. A. N. Tikhonov, "Inverse problems of heat conduction," Inzh.-Fiz. Zh., 29, No. 1, 7-12 (1975).
27. A. N. Tikhonov and V. Ya. Arsenin, Methods of Solving Incorrect Problems [in Russian], Nauka, Moscow (1974).
28. V. I. Zhuk and A. S. Golosov, "Engineering methods of determining thermal boundary conditions from data of temperature measurements," Inzh.-Fiz. Zh., 29, No. 1, 45-50 (1975).
29. L. A. Kozdoba, Solution of Nonlinear Problems of Heat Conduction [in Russian], Naukova Dumka, Kiev (1976).
30. Yu. M. Matsevityi, V. E. Prokof'ev, and V. S. Shirokov, The Solution of Inverse Problems of Heat Conduction with Electric Models [in Russian], Naukova Dumka, Kiev (1980).
31. D. F. Simbirskii, Temperature Diagnostics of Engines [in Russian], Tekhnika, Kiev (1976).
32. N. V. Shumakov, The Method of Successive Integrals in the Heat Measurement of Non-Steady-state Processes [in Russian], Atomizdat, Moscow (1979).
33. J. V. Beck and K. Arnold, Parameter Estimation in Engineering and Science, Wiley, New York (1977).
34. M. Imber, "Nonlinear problems of heat conduction in plane solids: direct and inverse problems," Raketn. Tekh. Kosmon., 18, No. 2, 96-107 (1979).
35. O. M. Alifanov, "Solution of the inverse problem of heat conduction by iteration methods," Inzh.-Fiz. Zh., 26, No. 4, 682-689 (1974).
36. O. M. Alifanov, "Determination of thermal loads from the solution of the nonlinear inverse problem," Teplofiz. Vys. Temp., 15, No. 3, 598-605 (1977).
37. O. M. Alifanov and S. V. Rumyantsev, "Stability of the iteration methods of solving linear incorrect problems," Dokl. Akad. Nauk SSSR, 248, No. 6, 1289-1291 (1979).
38. O. M. Alifanov and S. V. Rumyantsev, "Regularizing gradient algorithms for solving inverse problems of heat conduction," Inzh.-Fiz. Zh., 39, No. 2, 253-258 (1980).
39. O. M. Alifanov and S. V. Rumyantsev, "One method of solving incorrectly stated problems," Inzh.-Fiz. Zh., 34, No. 2, 328-331 (1978).

SHOCK WAVES IN A LIQUID CONTAINING VAPOR BUBBLES

R. I. Nigmatulin, V. Sh. Shagapov, N. K. Vakhitova, and Z. A. Shikhmurzaeva

UDC 532.529.5.533.6.011.72

The structure of shock waves in a liquid containing vapor bubbles is investigated, and an explanation is given for the mechanism of the anomalously high pressures in shock waves propagating in certain vapor–liquid media.

Condensation Shock

When a weak shock wave propagates in a liquid containing vapor bubbles, the temperature of the liquid does not change appreciably. Consequently, with the attendant increase in pressure and, hence, in the saturation temperature of the system the postshock vapor becomes supercooled, resulting in its condensation. Situations are therefore possible in which a shockwave reduces a two-phase mixture to a single-phase mixture.

Accordingly, the formulation of problems for bubbly liquids with allowance for the possibility of the annihilation of bubbles must incorporate sheets or boundaries $F^{(12)}$ separating regions of single- and two-phase flow. On these sheets $F^{(12)}$, which are aptly called condensation shocks, it is necessary to set up boundary conditions analogous to those on sheets of discontinuity.

We consider the stated conditions in a coordinate system wherein the sheet $F^{(12)}$ is at rest. The two-phase state (with bubbles) of the medium ahead of this shock is designated by the index 0, and the state of the medium

Institute of Mechanics, M. V. Lomonosov State University, Moscow. Bashkir State University, Ufa. Translated from Inzhenerno-Fizicheskii Zhurnal, Vol. 42, No. 2, pp. 192-206, February, 1982. Original article submitted July 24, 1981.

0022-0841/82/4202-0123$07.50

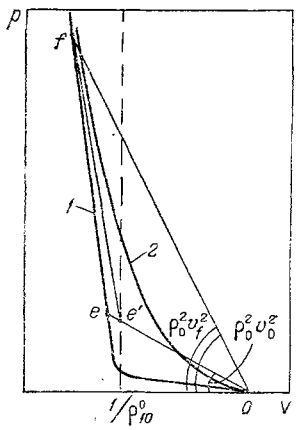

Fig. 1. Shock diagram for a bubbly vapor–liquid mixture.

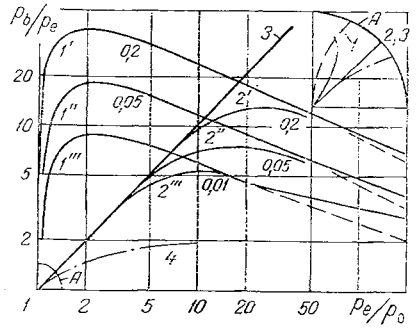

Fig. 2. Diagrams of the pressure intensification ratios for plane shocks reflected from a rigid wall. 1, 1', 1", 1"') steam–water mixture; 2, 2', 2", 2"') air–water mixture; 4) acoustic medium.

after the shock (in the form of a single-phase liquid) by the index e. Then the laws of conservation of mass, momentum, and energy, neglecting the mass, momentum, and energy of the bubbles in comparison with the same parameters for the liquid, acquire the form

$$\begin{gathered}\alpha_{10}\rho_{10}^0 v_0 = \rho_{1e}^0 v_e,\\ \alpha_{10}\rho_{10}^0 v_0^2 + p_0 = \rho_{1e}^0 v_e^2 + p_e,\\ \alpha_{10}\rho_{10}^0 v_0\left[\frac{v_0^2}{2} + k_{10} + u_{10}\right] + p_0 v_0 = \rho_{1e}^0 v_e\left[\frac{v_e^2}{2} + u_{1e}\right] + p_e v_e.\end{gathered} \tag{1}$$

Here k_{10} is the kinetic energy of small-scale radial motion per unit mass of liquid before the shock F[12]; α_{10}, volume content of liquid before the shock; u_{10}, v_0, p_0, specific internal energy of the liquid, the velocity, and the mean pressure of the medium before the shock; and u_{1e}, v_e, p_e, same parameters of the liquid after the shock; also,

$$p_0 = \alpha_{10}p_{10} + \alpha_{20}\left(p_{20} - \frac{2\sigma}{a_0}\right),\quad p_e = p_{1e},\quad \alpha_{20} = 1 - \alpha_{10}. \tag{2}$$

Knowing that the volume concentration of the bubbles is small ($\alpha_{20} \ll 1$), from now on we let $p_0 = p_{10}$, and for the pressure of the host liquid we assume a linear equation of state:

$$p_1 - p_0 = C_1^2(\rho_1^0 - \rho_{10}^0). \tag{3}$$

From the mass balance equation at the shock [first equation (1)] in conjunction with the equation of state (3) we deduce

$$\begin{gathered}\rho_{1e}^0 = \rho_{10}^0(1 + \alpha_c(P_e - 1)),\\ v_0 - v_e = v_0\alpha_{20}\frac{1 + (\alpha_c/\alpha_{20})(P_e - 1)}{1 + \alpha_c(P_e - 1)}\\ \left(\alpha_c = \frac{p_0}{\rho_{10}^0 C_1^2},\ P_e = \frac{p_e}{p_0}\right).\end{gathered} \tag{4}$$

Then from the equation of momentum conservation at the shock [second equation (1)] we obtain an expression relating the shock strength p_e to its velocity $D_0 = -v_0$ relative to the preshock (upstream) medium:

$$D_0^2 = v_0^2 = \frac{p_0}{\alpha_{10}\alpha_{20}\rho_{10}^0}(P_e - 1)\frac{1 + \alpha_c(P_e - 1)}{1 + (\alpha_c/\alpha_{20})(P_e - 1)}. \tag{5}$$

It is evident from this relation that the influence of the compressibility of the host liquid is embodied in the last cofactor. Thus, the compressibility of the liquid is insignificant, i.e., the entire compression of the mixture takes place through the bubbles if and only if

$$\delta_c = \frac{\alpha_c}{\alpha_{20}}(P_e - 1) = \frac{p_e - p_0}{\alpha_{20}\rho_{10}^0 C_1^2} \ll 1. \tag{6}$$

This condition holds for $\alpha_{20} \sim 10^{-1}$, $\rho_{10}^0 \sim 10^3$ kg/m^3, and $C_1 \sim 10^3$ m/sec if $p_e - p_0 \lesssim 10^2$ bar.

From the second equation (4) and from (5) we readily deduce an expression relating the velocity variation to the pressure at the condensation shock:

$$\Delta v_e = v_0 - v_e = \sqrt{\frac{\alpha_{20} p_0}{\alpha_{10}\rho_{10}^0}(P_e - 1)}\left(1 + \frac{\alpha_{10}}{2}\delta_c + O(\delta_c^2)\right). \tag{7}$$

From the energy equation at the shock [third equation (1)] we obtain

$$u_{1e} - u_{10} = k_{10} - \left[\frac{p_e}{\rho_{1e}^0} - \frac{p_0}{\rho_{10}^0\alpha_{10}} + \frac{v_e^2 - v_0^2}{2}\right]. \tag{8}$$

In cases where the influence of the compressibility of the host liquid is slight, i.e., where the inequality (6) or $|\rho_{1e}^0 - \rho_{10}^0| \ll \rho_{10}^0$ is valid, Eq. (8) can be rewritten

$$u_{1e} - u_{10} = k_{10} - \frac{\alpha_{20}}{\alpha_{10}}\frac{p_e}{\rho_{10}^0} + \frac{p_e - p_0}{\rho_{10}^0}\delta_c. \tag{9}$$

From the first and second equation (1) we readily obtain the relation

$$p_0 + (\rho_0 v_0)^2 \vartheta_0 = p_e + (\rho_0 v_0)^2 \vartheta_e, \tag{10}$$

$$\rho_0 = \rho_{10}^0\alpha_{10}, \quad \vartheta_0 = \frac{1}{\rho_0}, \quad \vartheta_e = \frac{1}{\rho_{1e}^0}.$$

Here ρ_0 is, with regard for the neglected mass of the bubbles, the mean density of the preshock mixture, and ϑ is the specific volume of the mixture.

A schematic shock diagram of a bubbly vapor–liquid mixture is shown in Fig. 1. Curve 1 is the shock adiabat of the mixture. The curve $p(\vartheta)$ has a very mild slope in the region of the original equilibrium ($k_{10} = 0$) two-phase state. This result is attributable to the fact that the vapor pressure in slow compression of a bubble scarcely increases, owing to condensation of the "excess" vapor mass. The slope of the curves at point 0 is determined by the equilibrium sound velocity $C^{(e)}$ sometimes called the Landau sound velocity [1], which is very small in such a mixture; in particular, it is much smaller than the same velocity in a mixture containing gas bubbles. When $\vartheta \approx 1/\rho_{10}^0$, i.e., when practically all the bubbles vanish, the compressibility of the medium is equal to that of the liquid, and so the diagram ostensibly acquires a sharp bend. It will be shown later that such a strong nonlinearity of the shock diagram induces a substantial increase in the pressure in the reflection of a wave or shock pulse of sufficient duration from a rigid wall. Curve 2 in Fig. 1 is the shock adiabat for a liquid containing gas bubbles of constant mass. The line 0e connecting the points corresponding to the preshock (0) and postshock (e) states of the mixture is called the Rayleigh–Michelson line. The slope of this line is determined by the factor $(\rho_0 v_0)^2$, i.e., by the shock velocity.

Reflection of the Condensation Shock from a Rigid Wall

Hereinafter we use the indices 0, e, and f to designate, respectively, the parameters ahead of the incident shock, after the incident and before the reflected shock, and after the reflected shocks. If the intensity of the incident shock is large enough to elicit complete condensation of the vapor, D_0 will be given by expression (5). Setting $v_0 = 0$, we can determine the particle velocity of the liquid after the incident shock from (7). Also,

$$\rho_{1f}^0 \approx \rho_{10}^0, \quad D_f \approx C_1,$$

because the reflected shock travels through a low-compressibility single-phase liquid, for which the curve $p(\rho^{-1})$ can be considered linear up to pressures $\sim 10^3$–10^4 bar.

In light of the foregoing we deduce an expression for the pressure after the reflected shock:

$$\frac{p_f}{p_e} = 1 + A_0 \frac{p_0}{p_e}\sqrt{\frac{p_e}{p_0} - 1}, \quad A_0 = \sqrt{\frac{\alpha_{20}}{\alpha_{10}}\frac{\rho_{10}^0 C_1^2}{p_0}}, \tag{11}$$

which indicates the degree of intensification of the shock wave in the vapor–liquid mixture upon relfection from a rigid wall in the case where the incident shock elicits complete condensation of the vapor and the compressibility of the liquid is felt only in the reflected shock. For comparison we give the corresponding relation for a gas–liquid system comprising a mixture of an incompressible liquid with gas bubbles of constant mass:

$$p_f/p_e = p_e/p_0 \tag{12}$$

and the relation for a low-compressibility linear acoustic medium:

$$\frac{p_f}{p_e} = 2 - \frac{1}{p_e/p_0}. \tag{13}$$

A diagram of the pressure ratio p_f/p_0 is given in Fig. 2 for plane shock waves reflected from a rigid wall in a steam–water mixture (curves 1, 1′, 1″, 1‴, $p_0=1$ bar, $T_0=373°K$), an air–water mixture (curves 2, 2′, 2″, 2‴, $p_0=1$ bar, $T=273°K$), and an acoustic medium (curve 4). The numbers 0.01, 0.05, and 0.2 indicate the values of the initial bubble concentration. The deviation of curve 1 from the dashed curve for small values of p_e/p_0 (view A) is associated with the incomplete condensation of the vapor after the shock. The deviation of curves 2, 2′, 2″, and 2‴ from the line 3 is associated with the advent of compressibility of the liquid in sufficiently strong shocks.

It is apparent from expression (11) and from Fig. 2 that a shock wave in a vapor–liquid mixture can be very greatly amplified in reflection. For example, in the case of a steam–water mixture with initial parameters $p_0=1$ bar, $\rho_{10}^0 \simeq 10^3$ kg/m^3, $C_1 \approx 1500$ m/sec, and $\alpha_{20}=0.1$ ($A_0^F=50$), after the reflection of waves with pressures $p_e=2$ bar and $p_e=5$ bar the pressures at the wall become equal to $p_f \approx 52$ and 105 bar, respectively. This amplification increases with the volume vapor concentration.

Structure of Time-Invariant Shock Waves

We consider the one-dimensional time-invariant motion of a liquid containing vapor bubbles under the usual conditions for two-phase monodisperse media [2, 3]. Following Nigmatulin [2], in the one-velocity approximation we write the equations of continuity and momentum for the mixture, the equations describing the laws of mass variation for a solitary bubble and a set of bubbles, and the equations for the variation of the bubble radius and radial motion of the liquid:

$$\frac{d}{dx}(\rho v) = 0, \quad \rho v \frac{dv}{dx} = -\frac{dp_1}{dx}, \quad v\frac{d}{dx}\left(\frac{4\pi}{3}a^3\rho_2^0\right) = 4\pi a^2 j,$$

$$\frac{d}{dx}nv = 0, \tag{14}$$

$$v\frac{da}{dx} = w_1 + \frac{j}{\rho_1^0}, \quad av\frac{dw_1}{dx} + \frac{3}{2}w_1^2 + 4\frac{\nu_1}{a}w_1 = \frac{p_2 - p_1 - \dfrac{2\sigma}{a}}{\rho_1^0}$$

$$\left(\rho = \rho_1^0(1-\alpha_2) + \rho_2^0\alpha_2, \ \alpha_2 = \frac{4}{3}\pi a^3 n\right).$$

Here $\rho, \rho_i, p_i, \alpha_i, w_i$ are the mean density of the mixture and the true density, pressure, volume concentration, and particle velocity of the i-th phase at the phase interface. In the last equation (equation of radial motion of the liquid) the differential pressure created at the bubble wall by phase transitions is neglected.

From now on we use the indices 1 and 2 to refer the parameters to the liquid and vapor phases, respectively.

An analysis of the behavior of a vapor bubble with an abrupt change of the pressure in the liquid shows [2, 4] that for temperatures and pressures of the medium not too close to the critical values the temperature nonuniformity of the vapor in the bubble interior is inconsequential. Then the thickness of the temperature boundary layer in the liquid is usually much smaller than the mean distance between the bubbles. Consequently, the heat and mass transfer around the vapor bubbles can be described by the heat-conduction equation for the liquid in the spherically symmetrical approximation; if we neglect the compressibility of the liquid, this equation has the form

$$\rho_1^0 c_1 \left(v \frac{\partial T_1}{\partial x} + w_r \frac{\partial T_1}{\partial r} \right) = \frac{1}{r^2} \frac{\partial}{\partial r} \left(r^2 \lambda_1 \frac{\partial T_1}{\partial r} \right), \quad w_r = \left(\frac{a}{r} \right)^2 w_1 \quad (0 < r < \infty). \tag{15}$$

At the interface ($r = a$) we specify the boundary conditions

$$T = T_s(p_2), \quad q_{\sigma 1} + q_{\sigma 2} = -jl, \quad q_{\sigma 1} = -\lambda_1 \frac{\partial T_1}{\partial r}, \quad \rho_1^0 \left(v \frac{da}{dx} - w_1 \right) = \rho_2^0 \left(v \frac{da}{dx} - w_2 \right) = j. \tag{16}$$

Under the condition of homogeneity of the pressure inside the bubble (homobaricity condition) [4] we can write the equation for the pressure in the vapor phase

$$v \frac{dp_2}{dx} = \frac{3(\gamma - 1)}{a} q_{\sigma 2} - \frac{3\gamma p_2}{a} w_2. \tag{17}$$

We further add the equations of state of the phases

$$p_1 = p_0 + C_1 (\rho_1^0 - \rho_{10}^0), \quad p_2 = \rho_2^0 R_2 T_2. \tag{18}$$

The system of equations (14) admits the first integrals

$$\rho v = \rho_0 v_0 = m_0, \quad nv = n_0 v_0, \quad p_1 + m_0 v = p_0 + m_0 v_0, \tag{19}$$

which express the conservation of the number of bubbles and the mass and momentum of the mixture. The additional subscript 0 refers to the parameters of the initial equilibrium state.

From the mass and momentum integrals (19) we readily obtain a one-to-one relation between the pressure and the density for a time-invariant shock wave:

$$p_1 + (\rho_0 v_0)^2 \vartheta = p_0 + (\rho_0 v_0)^2 \vartheta_0 \quad (\vartheta = 1/\rho). \tag{20}$$

It is evident from this expression that in a time-invariant shock wave the transition from state 0 to state e takes place along the Rayleigh–Michelson line.

For the ensuing discussion we write the equation for the variation of the kinetic energy of radial motion of the liquid per single bubble, deriving it from the equation of radial motion:

$$\frac{1}{a^2} \frac{dk_1}{da} = 2\pi \left(p_2 - p_1 - \frac{2\sigma}{a} \right) - 8\pi \frac{\rho_1^0 \nu_1}{a} w, \quad k_1 = 2\pi \rho_1^0 a^3 w^2 \quad (w = w_1). \tag{21}$$

Analysis of the System Under the Condition of Constant Pressure in the Bubble Interior

We analyze the system of differential equations given above for the case $p_2 = p_0$. This case obtains when the temperature of the bubble wall remains constant because of the large thermal conductivity of the liquid or because of continual restoration of the bubble wall by relative motion. Also, to economize on the calculations we neglect capillary effects, viscosity effects, the mass content of the vapor, and the density of the vapor in comparison with the density of the liquid. Then from Eqs. (16) and (14) we obtain

$$v = v_0 [1 - \alpha_{20} (1 - D^3)], \quad p_1 = p_0 + \rho_1^0 (1 - \alpha_{20}) v_0 (v_0 - v), \quad v \frac{da}{dx} = w, \quad av \frac{dw}{dx} + \frac{3}{2} w^2 = \frac{p_2 - p_1}{\rho_1^0} \left(p_2 = p_0, \ D = \frac{a}{a_0} \right), \tag{22}$$

whence we infer that

$$a \frac{d}{da} \left(\frac{w^2}{2} \right) + \frac{3}{2} w^2 = \alpha_{20} (1 - \alpha_{20}) v_0^2 (D^3 - 1). \tag{23}$$

The solution of the latter equation subject to the condition $w(a_0)=0$ has the form

$$w^2=\frac{\alpha_{20}(1-\alpha_{20})v_0^2}{3}(D^{-3/2}-D^{3/2})^2=\frac{p_e-p_0}{3\rho_1^0}(D^{-3/2}-D^{3/2})^2. \tag{24}$$

Then from the first and third equations (22) we have

$$\int_0^D \frac{1-\alpha_{20}(1-D^3)}{D^{-3/2}-D^{3/2}}\,dD=\frac{x}{a_0}[\alpha_{20}(1-\alpha_{20})/3]^{1/2}. \tag{25}$$

Here the constant of integration is determined from the condition $D=0$ at $x=0$. The first two relations from (22) and the resulting solutions (24), (25) determine the "structure" of the time-invariant shock wave in parametric form (with D as the parameter). The kinetic energy of radial motion of the liquid in the investigated process is expressed by the equation

$$k_1=\frac{2\pi\alpha_{20}(1-\alpha_{20})v_0^2a_0^3}{3}(D^{-3/2}-D^{3/2})^2D^3\rho_1^0. \tag{26}$$

From this relation we can find the quantity k_1 at the instant of bubble collapse ($D\to 0$):

$$k_{1f}=\frac{2\pi\alpha_{20}(1-\alpha_{20})v_0^2a_0^3\rho_1^0}{3}=\frac{4\pi}{3}a_0^3\frac{p_e-p_0}{2},$$

which has a finite value. If all of this kinetic energy is converted into heat after bubble collapse, the resulting increase in the temperature of the liquid mass m associated with a solitary bubble, estimated according to the equation

$$\Delta T=\frac{k_{1f}}{mc_1}=\frac{\alpha_{20}}{1-\alpha_{20}}\frac{p_e-p_0}{2\rho_1^0c_1}\left(m=\frac{4}{3}\pi a_0^3\rho_1^0\frac{1-\alpha_{20}}{\alpha_{20}}\right), \tag{27}$$

is usually negligible. The characteristic pressure increase $p'_e=p_e+\Delta p$ in the unit cell (associated with the solitary bubble) after bubble collapse can be estimated similarly, assuming that the entire kinetic energy of radial motion of the liquid mass m is converted at the instant of collapse into energy of elastic compression of the bubble:

$$k_{1f}=m\int_{p_e}^{p_f}\frac{p}{(\rho_1^0)^2}\,d\rho_1^0\approx m\frac{(p_f)^2-(p_e)^2}{2(\rho_{10}^0)^2C_1^2}. \tag{28}$$

Here, in computing the integral describing the work of the internal compression forces, we have taken into account the low compressibility of the liquid ($\rho_1^0-\rho_{10}^0\ll\rho_{10}^0$) and its acoustical equation of state. Substituting the values of m and k_{1f} into (28) and solving the resulting equation for p_f, we obtain

$$p_f=p_e\sqrt{1+\frac{p_e-p_0}{p_e}\frac{\rho_1^0C_1^2}{p_e}\frac{\alpha_{20}}{1-\alpha_{20}}}. \tag{29}$$

For example, if $p_e=2p_0=2$ bar, $\alpha_{20}=0.05$, and $C_1=1500$ m/sec, then $p_f\approx 30$ bar, corresponding to the magnitude of the oscillating pressure peaks in shock waves in experiments [5, 6].

We now estimate the influence of viscosity on the structure of a time-invariant shock wave on the basis of the solution obtained above. From Eq. (21), using the first and second relations (22) and relations (5), and neglecting the compressibility of the liquid and capillary effects, we obtain an expression for the kinetic energy of radial motion at the instant of bubble collapse:

$$k_{1f}=\frac{4\pi}{3}a_0^3\frac{p_e-p_0}{2}-k_\nu,\quad k_\nu=8\pi\rho_1^0\nu_1\int_{a_0}^{v}wada. \tag{30}$$

In (30) we can establish the following upper bound for the quantity k_ν expressing the viscosity-dispersed energy, making use of expression (24):

$$k_\nu<k_\nu^*=\frac{96\pi a_0^2\nu_1}{7}\left[\frac{\rho_1^0(p_e-p_0)}{3}\right]^{1/3}. \tag{31}$$

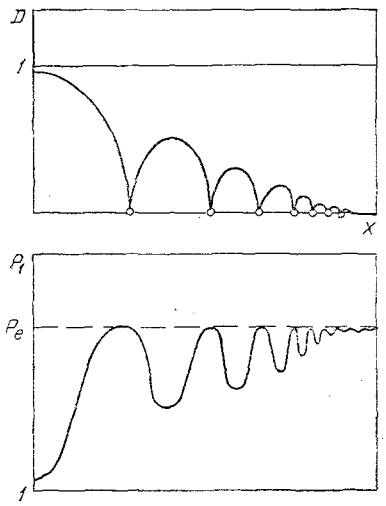

Fig. 3

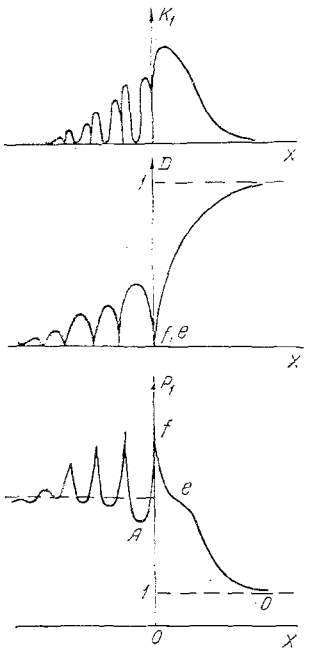

Fig. 4

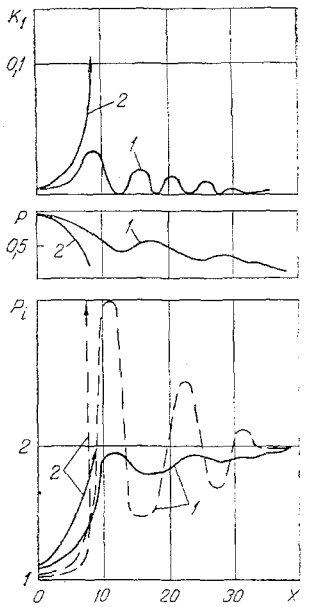

Fig. 5

Fig. 3. Structure of a time-invariant shock wave in the inertial regime of bubble collapse.

Fig. 4. Structure of a time-dependent shock wave in a bubble vapor–liquid mixture with oscillating pressure peaks induced by bubble collapse.

Fig. 5. Calculated curves for the structure of a time-invariant shock wave in a bubbly steam–water mixture.

Thus, for the kinetic energy of radial motion at the instant of bubble collapse we have the lower bound

$$k_{1f} > \frac{4\pi}{3} a_0^3 \frac{p_e - p_0}{2} \left(1 - \frac{144}{2\sqrt{3}} \frac{\nu_1}{a_0} \sqrt{\frac{\rho_1^0}{p_e - p_0}}\right). \tag{32}$$

For bubbles with radii $a_0 \approx 10^{-3}$–10^{-4} m in water the influence of viscosity can be neglected, and only in a very finely disperse mixture with $a_0 \sim 10^{-6}$ m can the viscosity have any appreciable influence.

For a low volume concentration of bubbles ($\alpha_2 \ll 1$) the motion of the latter relative to the liquid (two-velocity effect) has very little influence on the distribution of the parameters of the liquid ($p \approx p_1$, $v \approx v_1$), and so the given motion can be determined from the equation of motion of the bubbles according to the distribution of v and p_1 determined from the one-velocity approximation. If we neglect the viscosity of the liquid and take into consideration that the relative velocity of the phases is small, $|v_2 - v_1| \sim |v_0 - v_1| \ll v_0$, and the inertia of the bubble is determined by its additional mass, we obtain the equation of motion of the bubbles in the form [2, 3]

$$\frac{2\pi}{3} \rho_1^0 v_0 \frac{d}{dx}(a^3 v_{12}) = -\frac{4\pi}{3} a^3 \frac{dp}{dx} \quad (v \approx v_1 \approx v_0, \; v_{12} = v_1 - v_2, \; p \approx p_1). \tag{33}$$

Now, making use of the fact that the velocities of the phases coincide ahead of the shock wave, i.e., $v_{12} = 0$ at $a = a_0$, and invoking Eq. (24), we obtain

$$v_{12} = \alpha_{20}(1 - \alpha_{20}) v_0 (D^{-3} - D^3). \tag{34}$$

For the motion of the bubble relative to the liquid, using (24), we write

$$\Delta l = \int_{-\infty}^{x} \frac{v_{12}}{v_1} dx = \int_{a_0}^{a} \frac{v_{12}}{w} da = 2a_0 \sqrt{3\alpha_{20}(1 - \alpha_{20})} \left(\frac{1 - D^{1/2}}{D^{1/2}} - \frac{D^{5/2} - 1}{5}\right). \tag{35}$$

It is evident from this equation that the relative displacement increases with compression of the bubble. At a certain value of the radius a the displacement of the bubble relative to the liquid becomes commensurate with

the radius, so that the liquid at the surface of the bubble is replenished and heat transfer is intensified. Inasmuch as the heat- and mass-transfer rates in a liquid containing vapor bubbles are limited by the heat resistance of the liquid, ignoring the flow of liquid around the bubbles in Eqs. (15)-(17) will make the heat-transfer rate too low.

Calculation of the Structure of the Shock Wave with Radial Heat and Mass Transfer

Eliminating $q_{\sigma 2}$ by means of relations (16) and making use of the condition of conservation of the mass of the bubbles, i.e., the third equation (14), we write expression (15) in the form

$$v\frac{dp_2}{dx}+\left[\frac{(\gamma-1)l}{1-s}-\frac{\gamma p_2}{\rho_2^0}\right]v\frac{d\rho_2^0}{dx}=\frac{3(\gamma-1)}{a}\left(\lambda_1\frac{\partial T_1}{\partial r}\right)_a-\frac{3(\gamma-1)\rho_2^0 lw}{(1-s)a}\,(s=\rho_2^0/\rho_1^0). \tag{36}$$

It is important to note that this equation corresponds to the case in which the thermal diffusivity of the vapor is large enough to permit the temperature inside the bubble to follow the wall temperature. We can also analyze the opposite extreme of a small thermal diffusivity of the vapor, such that a uniform-temperature regime is realized. In this case the equation for p_2 follows from (17) for $q_{\sigma 2}=0$. Calculations have shown, however, that both extreme cases in the determination of p_1 yield practically the same results.

For numerical calculations we introduce the dimensionless variables

$$U=\frac{v}{a_*},\ W=\frac{w}{a_*},\ P=\frac{p}{p_0},\ \Phi_2=\frac{\rho_2^0}{\rho_{20}^0},\ \theta_1=\frac{T_1}{T_0},$$
$$X=\frac{x}{a_0},\ R=\frac{r}{a_0},\ K=\frac{k_1}{2\pi a_0^3 p_0},\ a_*=\left(\frac{p_0}{\rho_1^0}\right)^{1/2}.$$

After suitable transformations the system (14)-(18), (36) takes the form

$$U\frac{dD}{dX}=W,\ DU\frac{dW}{dX}=-\frac{3}{2}W^2+P_2-P_1-\frac{\sigma^*}{D}-\frac{\nu^*}{D}W,$$
$$U\frac{d\theta_1}{dX}=\frac{1}{R^2}\frac{\partial}{\partial R}\left(\lambda^* R^2\frac{\partial\theta_1}{\partial R}\right)-W\left(\frac{D}{R}\right)^2\frac{\partial\theta}{\partial R},$$
$$\frac{ADU}{3}\frac{dP_2}{dX}=\eta\lambda^*\left(\frac{\partial\theta}{\partial R}\right)_D-\frac{L\Phi_2 W}{1-s}, \tag{37}$$
$$U=U_0[1-\alpha_{20}(1-D^3)],\ P_1=1+\alpha_{20}(1-\alpha_{20})U_0^2(1-D^3),$$
$$P_2=\Phi_2\theta_s(P_2),\ K_D=D^3W^2,\ A=\frac{1}{\gamma-1}+\left[\frac{L}{(1-s)\theta_s}\frac{\gamma}{\gamma-1}\right](1-\Phi_2\theta_s'),$$
$$\theta_s'=\frac{d\theta_s}{dP_2}=\frac{\theta_s}{\Phi_2 L}\left(\sigma^*=\frac{2\sigma}{p_0a_0},\ \nu^*=\frac{8\nu}{a_*a_0},\right.$$
$$\left.\lambda^*=\frac{\lambda_1}{\rho_1^0c_1a_0a_*},\ \eta=\frac{\rho_1^0C_1}{\rho_{20}^0R_2},\ L=\frac{l\rho_{20}^0}{p_0}\right).$$

The penultimate member of this set of equations is the Clausius–Clapeyron equation in dimensionless form. For the numerical solution of Eqs. (37) it is necessary to analyze the asymptotic behavior of the solution of this system near the initial preshock equilibrium state. Accordingly, the system is linearized with respect to the values of the parameters at the point 0, and a solution is sought in the form of an exponential function decaying as $X\to-\infty$:

$$U=U_0+A_U\exp(KX),\ W=A_W\exp(KX),\ P_1=1+A_{P_1}\exp(KX), \tag{38}$$
$$\Phi_2=1+A_{\Phi_2}\exp(KX),\ D=1+A_D\exp(KX),\ \theta_1=1+A_{\theta_1}\exp(KX).$$

The condition for the existence of a solution in this form yields an equation for the determination of K.

It can be proved that the corresponding characteristic equation for K has one and only one positive root for $P_e<1$. In the case $P_e>1$ such a root does not exist. The system (37) therefore has a unique solution describing the structure of the compression shock.

The integral curves of the system of equations (37) admit translation along the X axis. We therefore fix a certain value of D at X = 0; D must be made close enough to unity for the linear solution to be valid in the region $X \leq 0$. The values of the other parameters at X = 0 are determined from the linear algebraic equations obtained by substituting a solution of the form (38) into the linearized system.

These quantities determine the initial conditions for the numerical solution of the nonlinear system of equations (37) in the region $X > 0$. To facilitate the numerical calculations we "freeze" the bubble radius by transforming to the new variable $\xi = R/D$ and reducing the heat-conduction equation to the form

$$U\frac{d\theta_1}{dX} = \left[\left(\frac{\xi}{D} - \frac{1}{\xi^2 D}\right)W + \frac{\lambda^*}{\xi D^2}\right]\frac{\partial\theta_1}{\partial\xi} + \frac{\lambda^*}{D^2}\frac{\partial^2\theta_1}{\partial\xi^2}. \tag{39}$$

The problem has been solved by a finite-difference procedure, where the exterior of the individual bubble is partitioned into spherical layers. The heat-conduction equation (39) goes over to a system of n ordinary differential equations. For the latter we arrive at the Cauchy problem, which has been solved on a computer by the Runge–Kutta method. The number of layers was varied, being chosen in such a way that its increment would have scarcely any influence on the results.

The preshock equilibrium state is associated with the point 0, which is a singularity of the system of differential equations. To avoid the singularity it is necessary to analyze the asymptotic behavior as $X \to -\infty$.

We can analyze the asymptotic behavior around the end state. By contrast with a liquid containing gas bubbles, where close to the final equilibrium state the system of differential equations admits a linear asymptotic representation, in the given case it is impossible to obtain the behavior of the solution involving bubble collapse in a finite analytical form. Numerical calculations show that for fairly weak shocks (for example, in the case of water with $p_0 \approx 1$ bar, $a_0 \approx 10^{-3}$ m, and $p_e/p_0 \leq 2$) the last stage of collapse takes place in the pure thermal regime, where the radial inertia of the liquid has virtually no effect and it can be assumed that $P_1 \approx P_2$. In this case, from the third equation in conjunction with the fourth and fifth relations (37) we obtain

$$\left[\frac{LP_2}{\theta_s(P_2)(1-s)} - A(P_e - 1)D^3\right]W = \eta\lambda^*\left(\frac{\partial\theta_1}{\partial R}\right)_D, \tag{40}$$

$$P_2 \simeq P_1 = 1 + (P_e - 1)(1 - D^3).$$

This equation must be solved simultaneously with the heat-conduction equation. If the compression process is sufficiently slow for the temperature distribution around the bubble to become restructured, acquiring the same profile as for steady-state heat transfer around a sphere:

$$\theta_1 = \frac{(\theta_s(P_2) - 1)}{R} + 1 \quad (\mathrm{Nu} = 2),$$

then from Eq. (40), neglecting D^3 terms in comparison with the end terms, we obtain

$$D^2 = \frac{2\eta\lambda^*(P_e - 1)X}{L^2 P_e U_e}. \tag{41}$$

From the above stated assumption underlying the validity of the given solution we deduce an estimate for the shock intensity:

$$p_e - p_0 \ll \Delta p_T = \frac{l}{c_1 T_0}\frac{\rho_2^0}{\rho_1^0}\rho_2^0 l.$$

For example, in the case of a steam–water mixture with $p_0 = 1$ bar we have $\Delta p_T = 0.025$ bar, i.e., the solution (41) is valid for very weak shock waves. For liquid nitrogen containing nitrogen vapor with $p_0 = 1$ bar and $T_0 = 77.3°K$ we have p = 0.1 bar.

Results of the Calculations and Conclusions

On the basis of the system of differential equations (37) we have carried out numerical calculations by the procedure described above. However, before presenting and discussing the results we consider the singular aspects of the behavior of the vapor bubbles with an increase in the pressure. The collapse of a vapor bubble is determined by the radial inertia and thermal conductivity of the liquid. It can have the nature of either accelerated collapse for $p_2 < p_1$ [in particular, similar to (26), when $p_2 = p_0$] or comparatively slow (monotonic or oscillating) gradual vanishing of the bubble for $p_2 \approx p_1$ [in particular, similar to (41)]. To assess the nature of

the collapse we can use the parameter B proposed in [7] (see also [2]), which is equal to the ratio of the characteristic collapse time $t' = a\sqrt{\rho_1^0/\Delta p}$ if it were limited only by the inertia of the liquid to the collapse time $t_T = a^2/(\nu_{1T} = Ja^2)$ $(\nu_{1T} = \lambda_1/\rho_1^0 c_1)$ if it were limited only by the thermal conductivity of the liquid $(B = t'/t_T)$. For large values of $B \gtrsim 10$ the process is limited by the inertia of the liquid and is close to the collapse acceleration regime (26) with a value of the kinetic energy of radial motion k_1 commensurate with k_{1f}. For small values of $B \lesssim 0.05$ the process is limited by the thermal conductivity of the liquid and has the nature of comparatively slow collapse if $k_1 \ll k_{1f}$.

When $B \ll 1$, the process does not manifest the compressibility of the host liquid, in which case $k_1 \approx 0$ and $p_1 \approx p_2$, and the transition from state 0 to state e takes place along the Rayleigh–Michelson line. In this case a time-invariant shock wave exists, its structure described by the solution of the system (37).

For $B \gg 1$ the inertial collapse regime in the state corresponding to the point e' (or close to it) prevails, and the kinetic energy of radial motion is finite. Consequently, the point e' in this case does not correspond to an equilibrium state. If the pressure in the liquid is determined from the condition of conversion of the kinetic energy of radial motion k_1 at the instant of bubble collapse into energy of elastic compression of the liquid, at which time the kinetic energy of radial motion becomes practically equal to zero, then the corresponding point f (see Fig. 1) on the shock adiabat converges with the Rayleigh–Michelson line. As a result, anomalous pressure spikes cannot be realized in the structure of the time-invariant shock wave. Consequently, the shock waves observed in the experiments of [5, 6] were strongly time-dependent. We now determine the shock velocity v_f corresponding to the maximum possible magnitude of the oscillating pressure peaks. For this velocity, which determines the slope of the Rayleigh–Michelson line joining the points 0 and f in Fig. 1, we obtain the following expression on the basis of relation (5) under conditions (6):

$$v_f = \left[\frac{p_f - p_0}{\rho_{10}^0 \alpha_{20}\alpha_{10}}\right]^{1/2} \approx \left\{\frac{[(p_e - p_0)\,\rho_{10}^0 C_1^2 \alpha_{20}/\alpha_{10}]^{1/2}}{\rho_{10}^0 \alpha_{20}\alpha_{10}}\right\}^{1/2} \approx \sqrt{v_0 C_1}.$$

Here we note that the velocity of a wave packet with the anomalously high pressure observed in the experiments of [5, 6] is satisfactorily consistent with this expression at the estimation level. The foregoing estimate clearly gives the value for the maximum velocity of propagation of the time-dependent part of the wave with high frequency oscillations initiated by the pressure p_e.

The structure of a time-invariant shock wave for $B \gg 1$ is shown schematically in Fig. 3. In this regime, where the bubbles experience a very great reduction from their initial dimensions and then expand, first of all, it is difficult in principle to calculate the wave structure from Eqs. (37) and, second, these equations are no longer justified. In particular, in the stage of collapse and subsequent expansion of the bubbles it is necessary to include the compressibility of the liquid, etc., in the equation of radial motion. However, inasmuch as these zones are of inconsequential extent, for the calculations they can be replaced by discontinuities at which the kinetic energy of the motion toward the center of the bubbles is converted with a certain degree of dissipation into kinetic energy of radial motion directed away from the center. These discontinuities are indicated by dots in Fig. 3.

As mentioned, strongly time-dependent shock waves have been observed in the experiments of [5, 6]. In the case dominated by the inertial collapse regime, with a minimal compression of the bubbles to retard their radial motion a drastic pressure increase must take place in the bubble interior, and, accordingly, the pressure will also increase in the equivalent cell [the maximum possible value of this increase is estimated by expression (29)], so that such time-dependent shock waves with anomalous high-frequency pressure peaks are realized for $B \gg 1$. The structure of such a time-dependent shock wave with a high-frequency oscillating "tail" is shown schematically in Fig. 4.

Realizations of the regime described here with anomalous pressure peaks can be promoted by the breakup of bubbles due to instability created by the reduction of their radii (in particular, this event causes the parameter B to increase). With growth of the bubbles and, hence, of the phase interface heat-transfer capacity of the liquid increases considerably, resulting in the accelerated collapse of bubbles with a finite value of k_1.

A problem still outstanding is the quantitative theoretical description of the structure of a time-dependent shock wave with an oscillating packet, in which the medium goes over to a single-phase equilibrium state after executing several oscillations with the dissipation of kinetic energy and the multiple diminution as well as almost complete vanishing of bubbles, with regard for the effects of compressibility of the liquid and bubble breakup.

The maximum amplitude of the oscillations is estimated by expression (29) and, as noted above, is reasonably consistent with the experimental data. The most complicated problem is to predict the lifetime of the oscillations or of the oscillating tail. This problem can be significant, because the collapse of vapor bubbles is accompanied by quite a few oscillations, and the tail of the wave can be very long.

In light of the indicated considerations, the feasibility of establishing the time-invariant shock structure shown schematically in Fig. 3 in a liquid containing vapor bubbles also poses an intricate fundamental problem. Only with continued detailed experimental and theoretical studies will an answer be forthcoming.

Below, we analyze the results of calculations performed on the basis of the equations discussed above. All of the thermophysical properties are taken from [8]. Figure 5 shows the structure of a shockwave for water containing vapor bubbles with the following values of the parameters governing the initial state of the mixture, the wave intensity P_e, and its velocity v_0 relative to the preshock medium: $\alpha_{20}=0.05$; $p_0=1$ bar; $a_*=10$ m/sec; $P_e=2$; $v_0=45.9$ m/sec. Curve 1 is calculated for a bubble diameter $2a_0=10^{-3}$m, and curve 2 for $2a_0=10^{-4}$ m. It is evident from the graph that for bubbles with $2a_0=10^{-3}$ m the parameters (pressures of the phases P_1 and P_2 and the diameter 2a) execute several oscillations and in the monotonic regime tend to their limiting postshock values. The kinetic energy of radial motion at first has two or three oscillations and then tends to zero. Thus, a time-invariant shock wave exists for the given situation. As noted above, Eq. (37) makes the heat-transfer rate too low, because the given model ignores slip of the bubbles relative to the liquid and bubble breakup effects. The effects of slip [with the use of (35)] and breakup can be estimated against the background of the numerical solution.

The displacement of the bubbles relative to the liquid during the first maximum compression ($D\approx0.4$) is equal to $\Delta l\sim0.6$. Thus, the possible maximum displacement is approximately one third the first minimum value of the diameter, i.e., the surface of the bubble cannot be restored, and the slip effect can be neglected.

Bubble breakup can be induced, first, by dynamic differentials created in the gaseous phase during relative motion of the phases and, second, by retardation of the radial motion of the bubble boundaries in connection with the increase of the vapor pressure inside the bubbles as they are compressed.

The conditions for bubble breakup initiated by the above-noted effects take the respective forms [8]

$$\frac{\rho_2^0 v_{12}^2 a}{\sigma} = W_e > W_e^* \simeq \pi, \tag{42}$$

$$\frac{\rho_1^0 g a^2}{\sigma} = B_0 > B_0^* = \pi^2. \tag{43}$$

Here g is the acceleration of the liquid at the phase interface during radial motion of the bubbles.

It is evident from expressions (42) and (43) that surface tension inhibits breakup in both cases.

With the use of expression (34) for v_{12}, condition (42) can be written in the form of a relation determining the dimensionless bubble radius (D) at which breakup is possible:

$$(D^{-3}-D^3)\,D \gtrsim B_1,\quad B_1=\frac{4\pi\sigma}{(\alpha_{20}v_0)^2\rho_2^0 a_0}=\frac{4\pi\sigma\rho_1^0}{(p_e-p_0)\,\alpha_{20}\rho_2^0 a_0}. \tag{44}$$

An analysis of this relation in application to the given example shows that the condition for breakup by dynamic differentials is expressed by the inequality $D \lesssim 0.05$.

In the given problem, however, $D\simeq0.4$ in the first maximum compression. Thus, the dynamic differentials of the gaseous phase in the given case apparently do not elicit bubble breakup. For the given example condition (42) holds in the first compression of the bubbles in the wave, indicating the possibility of bubble breakup induced by retardation of the radial motion of their boundaries on the vapor side. An analysis of the experiments of [10, 11] shows that the same effect is responsible for the instability of air bubbles in the case of waves with $P_e\approx2$-3.

The results of the calculations indicate that when a shock wave propagates in a mixture containing small bubbles it is possible for "anomalously" large pressures to be created. The occurrence of such pressure peaks in a disperse mixture containing "large" bubbles can be attributed to their breakup in the initial stage of shock compression. The breakup process in the initial stage has the effect of making the propagation of a shock wave in a mixture with "large" bubbles equivalent to the propagation of a wave of the same intensity, but in a mixture containing indivisible "small" bubbles. The factors responsible for breakup can be ascertained by means of the criteria (42) and (43).

The tendency toward the realization of strong high-frequency pressure "spikes" in a shock wave with a reduction of the initial bubble diameter is attributable to the reduction of the heat resistance between the phases as a result of the growth of the specific phase interface.

We have carried out calculations for liquid nitrogen containing nitrogen bubbles with the following parameters governing the initial state of the mixture and the shock intensity: $\alpha_{20}=0.05$; $p_0=1$ bar; $P_e\approx 2$-3; $2a_0=10^{-3}$ m. For media whose initial state and shock intensity are close to these values, the amplification of shock waves has been observed in experiments [5], even though calculations without regard for breakup predict that a time-invariant shock wave must exist in these cases. Clearly, for these parameters a spontaneous decomposition of bubbles into smaller bubbles takes place at the shock front, where it is induced predominantly by the relative motion of the phases. The probability of breakup by this mechanism in the case of nitrogen bubbles is greater than for water bubbles due to the roughly tenfold decrease in the parameter B_1 governing the threshold of instability. The latter result is attributable to the fact that, because of the low temperature ($T_0=77°K$, $\rho_2^0=5$ kg/m^3), the density of nitrogen vapor is an order of magnitude greater than that of steam ($T_0=373°K$, $\rho_2^0=0.6$ kg/m^3).

We note once again that the breakup of bubbles by a shock wave into a set of much smaller fragments is probably attributable in large part to Kelvin–Helmholtz instability. This conjecture is also evinced, in particular, by the results of [9]. We infer from the foregoing discussion that the tendency toward anomalous pressures is dictated by the heat resistance of the liquid and depends on the thermal diffusivity of the liquid, the bubble sizes, and the possibility of breakup into much smaller fragments.

NOTATION

ρ_1^0, ρ_2^0, true densities of the liquid and vapor; v, velocity; p_1, p_2, mean pressure in the liquid phase and pressure in the bubbles; α_2, volume concentration of bubbles; n, number of bubbles per unit volume; a, bubble radius, w_1, w_2, particle velocities of radial motion of the liquid and vapor at the phase interface; k_1, kinetic energy of bubble motion; j, interphase mass-transfer rate per unit area of the phase interface; $q_{\sigma 1}$, $q_{\sigma 2}$, heat fluxes per unit area of the phase interface in the liquid and in the vapor; ν_1, σ, viscosity and coefficient of surface tension of the liquid; l, specific heat of vaporization; c_1, λ_1, specific heat and thermal conductivity of the liquid; γ, adiabatic exponent of the vapor; $T_s(p_2)$, vapor saturation temperature at pressure p_2; C_1, sound velocity in the liquid phase; B, gas constant; Φ, V, P, D, W, θ, K_1, dimensionless values of the vapor density, velocity, pressure, radius, radial particle velocities of the phases, temperature, and kinetic energy; $a_*=\sqrt{p_0/\rho_{10}^0}$, characteristic velocity; $\sigma^*=2\sigma/p_0a_0$, $\nu^*=8\nu_1/a_*a_0$, $\lambda^*=\lambda_1/(\rho_{10}^0c_1a_*a_0)$, $\eta=\rho_{10}^0c_1/\rho_{20}^0B$, $L=l\rho_{20}^0/p_0$, characteristic dimensionless parameters. Indices: 0, e, preshock and postshock equilibrium states.

LITERATURE CITED

1. L. D. Landau and E. M. Lifshits, Continuum Mechanics [in Russian], Tekhizdat, Moscow (1954).
2. R. I. Nigmatulin, Fundamentals of the Mechanics of Heterogeneous Media [in Russian], Nauka, Moscow (1978).
3. R. I. Nigmatulin and V. Sh. Shagapov, "Structure of shock waves in a liquid containing gas bubbles," Izv. Akad. Nauk SSSR, Mekh. Zhidk. Gaza, No. 6, 30-41 (1974).
4. R. I. Nigmatulin and N. S. Khabeev, "Dynamics of vapor–gas bubbles," Izv. Akad. Nauk SSSR, Mekh. Zhidk. Gaza, No. 6, 56-61 (1976).
5. A. A. Borisov, V. E. Gel'fand, and A. A. Gubaidullin, "Amplification of shock waves in a liquid containing gas bubbles," in: Nonlinear Wave Processes [in Russian], Novosibirsk (1977), pp. 67-74.
6. B. E. Gel'fand, V. V. Stepanov, E. I. Timofeev, and S. A. Tsygankov, "Amplification of shock waves in a nonequilibrium medium comprising a liquid and dissolved gas bubbles," Dokl. Akad. Nauk SSSR, 339, No. 1, 71-74 (1978).
7. L. W. Florscheutz and T. Claob, "On the mechanics of vapor bubble collapse," Trans. ASME, Ser. C: J. Heat Transfer, 87, No. 2, 209-220 (1965).
8. N. B. Vargaftik, Tables on the Thermophysical Properties of Liquids and Gases, 2nd ed., Halsted Press (1975).
9. B. E. Gel'fand, S. A. Gubin, R. I. Nigmatulin, and E. I. Timofeev, "Influence of the gas density on the breakup of bubbles by shock waves," Dokl. Akad. Nauk SSSR, 235, No. 2, 292-294 (1977).
10. L. Noordzij, "Shock waves in bubble-liquid mixtures," Phys. Commun. Twente Univ. Tech., 3, No. 1, 52 (1971).
11. S. S. Kutateladze, A. P. Burdukov, V. V. Kuznetsov, et al., "Structure of a weak shock wave in a gas–liquid medium," Dokl. Akad. Nauk SSSR, 207, No. 2, 313-315 (1972).